A redox switch in C-reactive protein modulates activation of endothelial cells

Ming-Yu Wang,[*,†,1] Shang-Rong Ji,[*,†,1] Cai-Juan Bai,[*,†] Driss El Kebir,[‡] Hai-Yun Li,[*,†] Jing-Ming Shi,[*,†] Wei Zhu,[*,†] Santiago Costantino,[‡] Hai-Hong Zhou,[*,†] Lawrence A. Potempa,[§] Jing Zhao,[*,†] János G. Filep,[‡,2] and Yi Wu[*,†,2]

*Ministry of Education Key Laboratory of Arid and Grassland Ecology, Institute of Biophysics, and †Second Hospital, Lanzhou University, Lanzhou, China; ‡Research Center, Maisonneuve-Rosemont Hospital, University of Montréal, Montréal, Québec, Canada; and §Roosevelt University College of Pharmacy, Schaumburg, Illinois, USA

ABSTRACT   C-reactive protein (CRP) has been implicated in the regulation of inflammation underlying coronary artery disease; however, little is known about the molecular mechanisms responsible for the expression of its pro- or anti-inflammatory activities. Here, we have identified the intrasubunit disulfide bond as a conserved switch that controls the structure and functions of CRP. Conformational rearrangement in human pentameric CRP to monomeric CRP (mCRP) is the prerequisite for this switch to be activated by reducing agents, including thioredoxin. Immunohistochemical analysis revealed 36–79% colocalization of thioredoxin and mCRP in human advanced coronary atherosclerotic lesions. Nonreduced mCRP was largely inert in activating human coronary artery endothelial cells (HCAECs), whereas reduced or cysteine-mutated mCRP evoked marked release of IL-8 and monocyte chemoattractant protein-1 from HCAECs, with ~50% increase at a concentration of 1 µg/ml. Reduced mCRP was ~4 to 40-fold more potent than mCRP in up-regulating adhesion molecule expression, promoting U937 monocyte adhesion to HCAECs, and inducing cytokine release from rabbit arteries *ex vivo* and in mice. These actions were primarily due to unlocking the lipid raft interaction motif. Therefore, expression of proinflammatory properties of CRP on endothelial cells requires sequential conformational changes, *i.e.*, loss of pentameric symmetry followed by reduction of the intrasubunit disulfide bond.—Wang M-Y., Ji, S-R., Bai, C-J., El Kebir, D., Li, H-Y., Shi, J-M., Zhu, W., Costantino, S., Zhou, H-H., Potempa, L. A., Zhao, J., Filep, J. G., Wu, Y. A redox switch in C-reactive protein modulates activation of endothelial cells. *FASEB J.* 25, 000–000 (2011). www.fasebj.org

C-REACTIVE PROTEIN (CRP), one of the prototypic human acute-phase reactants, plays important roles in host defense and inflammation (1–2). Accumulating evidence indicates that CRP is not merely a predictor, but rather a mediator of acute cardiovascular disease (1–3). However, apparently contradictory results considerably hampered defining the precise role of CRP in atherogenesis and plaque vulnerability. For example, transgenic expression of human CRP or knockout of endogenous CRP in atherosclerosis-prone mice has been reported to accelerate (4), not to affect (5), or even to protect against atherosclerosis development (6–7). Transgenic expression of human CRP in rabbits did not promote lesion formation (8). In addition, considering the proinflammatory actions of CRP on endothelial cells and leukocytes, it is unclear how the body adapts to the dynamic fluctuations in plasma CRP level in the range of 2–3 orders of magnitude (1). These enigmas could be explained by the existence and controlled formation of different CRP isoforms (2, 9–11).

CRP has two conformationally distinct isoforms, *i.e.*, circulating pentameric CRP (pCRP), composed of 5 identical subunits, and tissue-associated monomeric CRP (mCRP), formed by dissociation of pCRP subunits or produced directly by extrahepatic cells (12). The overall effects of pCRP appear to be anti-inflammatory (9–10), whereas mCRP possesses potent proinflammatory actions on endothelial cells (13), neutrophils (14), platelets (15), and monocytes (16). Moreover, conversion of pCRP to mCRP in the inflammatory microenvironment (9, 16–17) could restrict the proinflammatory effects of CRP at the sites of tissue injury. These findings lead to the concept that mCRP is the major isoform amplifying local inflammatory responses, while pCRP may serve as the precursor of mCRP as well as a marker of inflammation.

At present, little is known about how the structure of CRP may affect its biological activities. Indeed, large variations in endothelial cell responses to CRP under

---

different experimental conditions (13, 18–19) imply a yet unidentified control mechanism. Here, we report that the intrasubunit disulfide bridge functions as a conserved redox-sensitive switch in CRP, the functionality of which requires conversion of pCRP to mCRP. We also show that thioredoxin (Trx), a ubiquitous reducing enzyme that is critical for thiol/disulfide redox homeostasis (20–21), frequently colocalizes with mCRP in human advanced coronary artery plaques and reduces the disulfide bridge in mCRP. Reduced mCRP exhibits more potent proinflammatory actions on human coronary artery endothelial cells (HCAECs) *in vitro*, on rabbit blood vessels *ex vivo*, and in mice. We propose that the highly controlled interplay between different structural conformations underlies the intrinsic properties of CRP as fine modulator of inflammation, thereby linking endothelial cell dysfunction and microenvironment redox status to coronary artery disease.

MATERIALS AND METHODS

Reagents

Human native pCRP (purity >99%) was purified from ascites or purchased from BindingSite (Birmingham, UK). mCRP was produced by dissociation of pCRP in 8 M urea-EDTA (22), low-pH EDTA (22), or low-salt buffer-EDTA (23–24). Cysteine (Cys)-mutated mCRP was prepared as described previously (17, 24–25). In this mutant, the two Cys were replaced with alanine (Ala). Rabbit pCRP and mCRP were prepared as described previously (23, 26). Proteins were dialyzed to remove NaN$_3$, assayed for endotoxin contamination by the *Limulus* assay (Sigma-Aldrich, St. Louis, MO, USA), and passed through Detoxi-Gel columns (Thermo Fisher Scientific, Rockford, IL, USA) to remove endotoxin when necessary. The endotoxin level in all protein solutions was below the detection level (0.06 EU/ml) of the *Limulus* assay. Mouse anti-human mCRP and pCRP mAbs were generated as described previously (27). Reagents were purchased from Sigma-Aldrich unless otherwise stated.

We have used 2 methods to reduce the intrasubunit disulfide bridge in mCRP. In the first method, 5 mM dithiothreitol (DTT) was present during the preparation of mCRP from pCRP by urea-EDTA. To prevent spontaneous reoxidation, reduced mCRP was dialyzed into a buffer containing 0.1 mM DTT. This procedure resulted in complete reduction of the disulfide bridge in mCRP. In the alternative method, preformed mCRP was incubated with reducing agents [DTT, glutathione (GSH), or Cys] or Trx immediately before the binding or cell-stimulation assays. This method yielded partially reduced mCRP (**Fig. 1**).

Sodium dodecylsulfonate-polyacrylate gel electrophoresis (SDS-PAGE) and immunoblotting

Reduced and nonreduced mCRP samples were analyzed by 12% nonreducing SDS-PAGE, in which the reduced subunit ran slower than the nonreduced subunit. Before electrophoresis, 50 mM *N*-ethylmaleimide (NEM) was added to quench the reducing reaction and to prevent the reoxidation of the free thiols during electrophoresis. To minimize structural disturbance, samples were not heated (19). The bands were visualized by silver staining. For Trx-reduced mCRP, samples were transferred to PVDF membranes and probed with 3H12 mAb against mCRP or a sheep anti-human CRP polyclonal antibody (BindingSite). The content of reduced mCRP was calculated as the band intensity of reduced mCRP/(band intensity of reduced mCRP + band intensity of nonreduced mCRP) × 100%.

Assessment of protein conformation

Circular dichroism (CD) spectra were recorded on a Jasco 810 spectrophotometer (Jasco, Easton, MD, USA) to determine changes in the secondary structure of mCRP. Intrinsic fluorescence (excitation: 280 nm; emission: 345 nm) and 8-anilino-1-naphthalenesulfonate (ANS; Sigma-Aldrich) fluorescence (excitation: 380 nm; emission: 480 nm) were collected on an LS-55 spectrofluorometer (PerkinElmer, Waltham, MA, USA) to measure changes in the tertiary packing of mCRP. ANS is nonfluorescent in polar solvents but shows significant increase in fluorescence following binding to protein hydrophobic regions. A 20-fold molar excess of ANS was incubated with the samples for 30 min in the dark. The influence of DTT in the range of intrinsic fluorescence emission was assessed and corrected by using Cys-mutated mCRP.

In-gel digestion and mass spectrometry

Following separation by nonreducing SDS-PAGE, the bands corresponding to reduced and nonreduced mCRP were excised. After washing and drying, in-gel digestion was accomplished by trypsin (Promega, San Luis Obispo, CA, USA) treatment for 16 h at 37°C. The digested mCRP peptides were extracted and analyzed with a matrix-assisted laser desorption/ionization time of flight (MALDI-TOF) mass spectrometer (Kompact MALDI IV; Shimadzu, Hong Kong, China) equipped with a nitrogen laser (337 nm) at acceleration energy of 20 kV. All spectra were acquired in linear negative mode, and the peptide peaks were identified by the DeNovo software (DeNovo Software, Los Angeles, CA, USA) using the Swiss-Prot database.

Ligand interactions

The C1q binding (25), C3 activation (25), LDL binding (24), and lipid monolayer insertion assays (24, 28) were performed as described previously. Briefly, reduced or nonreduced FITC-labeled mCRP was added to C1q- or LDL-coated wells for 1 h at 37°C, and mCRP binding was determined by fluorescence intensity and expressed as nanograms of protein bound. mCRP-ligand interactions were also evaluated by using fluid-phase ligands and immobilized mCRP. Antibodies against C1q or LDL (Sigma-Aldrich) were used to determine the binding to mCRP. For C3 activation, 2% normal human serum (NHS) was added to mCRP-coated wells for 1 h at 37°C. C3d deposition was detected by a sheep anti-human C3d polyclonal antibody (BindingSite). For monolayer insertion, protein was injected beneath the lipid monolayer composed of egg phosphatidylcholine:sphingomyelin:cholesterol (mol/mol/mol, 1:1:1), which resembles the composition of lipid raft in cell plasma membrane. Membrane insertion was monitored by increases in surface pressure.

Endothelial cell responses

HCAECs (Cell Applications, San Diego, CA, USA) were cultured as described previously (17). Confluent HCAEC (at passages 4 to 6) monolayers in 96-well microplates were
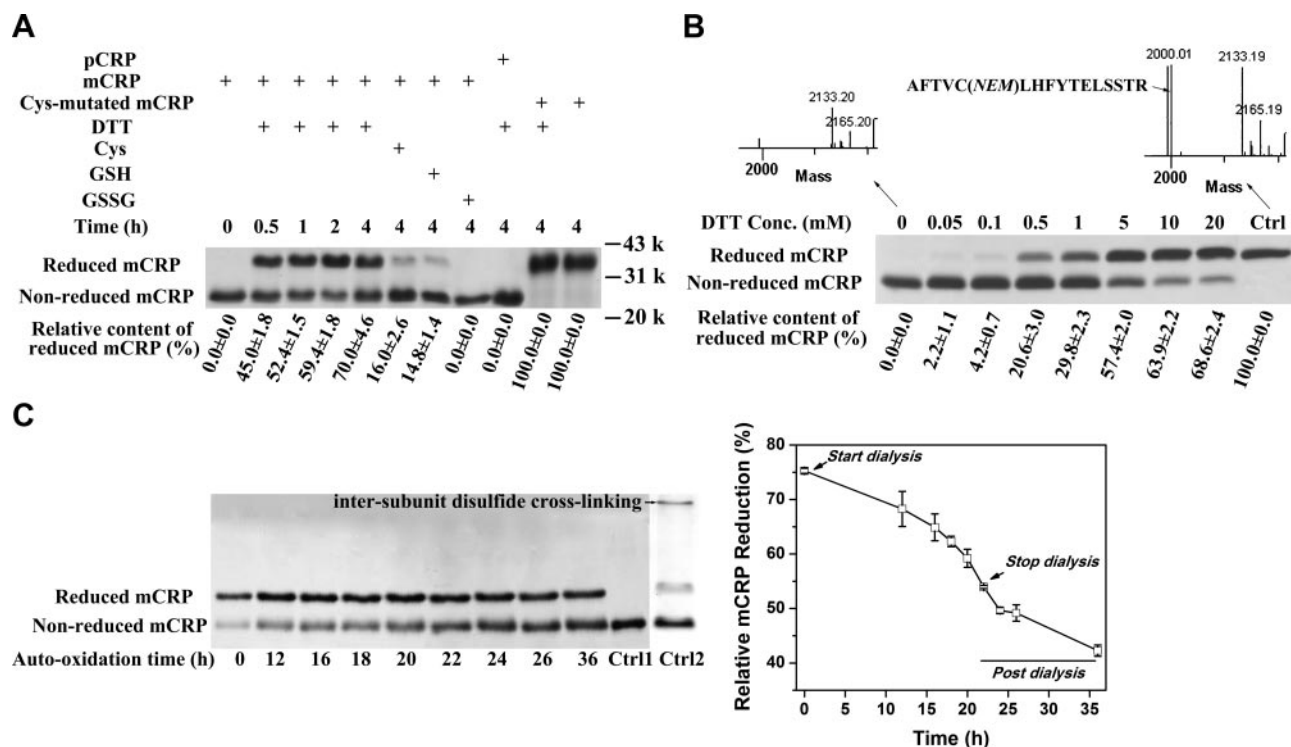
Figure 1. Intrasubunit disulfide bond is redox sensitive in mCRP but not pCRP. Samples were treated with NEM to block free thiols of proteins and residue-reducing agents, and then subjected to nonreducing SDS-PAGE. Content of reduced mCRP was calculated as the band intensity of reduced mCRP/(band intensity of reduced mCRP + band intensity of nonreduced mCRP) × 100%. *A)* mCRP, pCRP, or Cys-mutated mCRP was treated with 5 mM DTT or 20 mM Cys, GSH or GSH-disulfide (GSSG) for indicated times. During the assay, 2 mM Ca^{2+} was present to prevent spontaneous dissociation of pCRP. *B)* mCRP was treated with increasing concentrations of DTT for 2 h at 37°C, diluted with nonreducing sample buffer, and subjected to SDS-PAGE without heating. Heat-treated (100°C, 5 min) mCRP in reducing loading buffer served as control. Bands corresponding to reduced and nonreduced mCRP were in-gel trypsinized, extracted, and analyzed by mass spectrometry. Presence of the finger peptide aa 32–47 with Cys modified with NEM was observed only for reduced mCRP. Full spectra are included in Supplemental Fig. S1. *C)* DTT (10 mM)-treated mCRP was incubated at room temperature to assess the autooxidation or spontaneous reformation of the intrasubunit disulfide bond. First 22 h incubation was conducted under dialysis conditions to remove DTT. Untreated mCRP served as nonreduced control (Ctrl 1). Intersubunit disulfide cross-linking could be visualized only following a combination of autooxidation and unfolding treatments (Ctrl 2).

cultured with mCRP for 4 h. Interleukin (IL)-8 and monocyte chemoattractant protein (MCP)-1 concentrations in conditioned medium were determined by commercial ELISA kits (BD Pharmingen, San Diego, CA, USA) (17). Cell surface expression of vascular cell adhesion molecule-1 (VCAM-1), intercellular adhesion molecule-1 (ICAM-1) and E-selectin (BD Pharmingen) were determined by immunofluorescence (17). Nonspecific binding was evaluated by use of isotype-matched irrelevant mouse IgG. For detection of reactive oxygen species (ROS), HCAECs were stimulated for 2 h. After 2 washes, HCAECs were incubated with 10 μM dichlorodihydrofluorescein diacetate (H2DCF-DA; Invitrogen, Carlsbad, CA, USA) for an additional 30 min; fluorescence was measured in a Biotek Synergy HT plate reader (Biotek Instruments, Winooski, VT, USA). Cell-associated ROS were visualized by Leica DM5000B fluorescence microscope (Leica Microsystems, Wetzlar, Germany). For monocyte adhesion, 100 μl phorbol myristate acetate (PMA)-activated U937 monocytes (5×10^5/ml) were added to HCAEC monolayers for 30 min. The wells were gently washed 3 times, and HCAECs together with the attached monocytes were stained with crystal violet. Attached monocytes were counted in 5 randomly photographed fields. To exclude possible confounding effects from endotoxin, all experiments were performed in the presence of 20 U/ml polymyxin B. The residue concentrations of reducing agents during the functional

assays were <0.25 mM for DTT and <1 mM for GSH and Cys. Our preliminary data showed that the reducing agents at these concentrations did not affect HCAEC responses.

Cytokine release from rabbit thoracic aortas *ex vivo*

Thoracic aortas dissected from New Zealand rabbits were cultured for 16 h in RPMI 1640 supplemented with 5% fetal bovine serum (FBS) at 37°C in 5% CO_2 atmosphere. The vessels were incubated with 50 μg/ml mCRP or reduced mCRP for 4 h. IL-8 released from blood vessels was determined by ELISA kit (Westang, Shanghai, China) and normalized by vessel size.

Cytokine release in mice

Male Kunming mice (20–25 g) were injected intraperitoneally with vehicle or with mCRP or reduced mCRP at 2.5 mg/kg body weight. Reduced mCRP and mCRP were prepared from pCRP by urea-EDTA in the presence or absence of 5 mM DTT, respectively. This protocol yielded nearly complete mCRP reduction and minimized the amounts of reducing agent injected into the animals. At 2 h postinjection, the animals were anesthetized with ether, and the peritoneum was perfused with 500 μl PBS. Perfusate IL-6 and IL-10

levels were determined by specific ELISA kits (Westang). The experimental protocols were in accordance with the policies of Lanzhou University.

Immunohistochemistry

Human archival coronary artery specimens were obtained from the Tissue Bank at the Montreal Heart Institute (Montreal, QC, Canada). The Clinical Research and Ethics Committees at the Tissue Bank (CERICM 08-1063) and the Maisonneuve-Rosemont Hospital (CER-08011) approved the experimental protocols. Aortic segments were frozen in optimal cutting temperature (OCT) compound (Sakura Finetek, Torrance, CA, USA) or embedded in paraffin and stored at −80°C. Atherosclerotic lesions were classified according to the American Heart Association. Patient characteristics are reported in Supplemental Table S1. Specimens were cut into 6-μm serial sections, immobilized on precleaned microscope slides, and thawed at room temperature for 30 min, followed by fixation in acetone (−20°C for 20 min), 10% buffered formalin (2 min at room temperature), and absolute ethanol (10 min at room temperature). Immunohistochemical detection was done with a Discovery XT immunostainer (Ventana Medical Systems, Tucson, AZ, USA) performing deparaffinization and antigen retrieval with proprietary reagents. Slides were treated with anti-human CRP antibody clone 8D8, anti-human mCRP antibody clone 9C9 (both used as tissue-culture supernatant in a 1:50 dilution; ref. 7), mouse anti-human Trx antibody clone 2B1 (ABD Serotec, Oxford, UK), or mouse IgG isotype-matched control (ABD Serotec) for 60 min, and then incubated with a biotinylated anti-mouse IgG (Vector Laboratories, Burlingame, CA, USA) for an additional 30 min. Subsequently, slides were incubated with an anti-avidin-biotin-peroxidase system, and the reaction products were stained with DAB substrate kit (DABmap kit, Ventana Medical Systems) for CRP and mCRP or Fast Red kit (Redmap kit, Ventana Medical Systems) for Trx. Double immunostaining was performed on some slides by sequentially staining for mCRP and Trx. Slides were then counterstained with hematoxylin, mounted, and scanned at ×40 magnification using the C9600 NanoZoomer System (Hamamatsu Photonics K.K., Hamamatsu, Japan), which is capable of adjusting focus on any part of the slide. Virtual slides were visualized and analyzed with the NDP Scan 2.0 software (Hamamatsu Photonics) and digital pictures were taken to illustrate antibody localization.

Assessment of colocalization of mCRP and Trx

Color stains in the image were separated using color deconvolution (29). The RGB components of each stain were determined by manually selecting areas of the image where they did not seem to mix using ImageJ (U.S. National Institutes of Health, Bethesda, MD, USA). A linear equation system for each pixel in the image was used to determine the amounts of each of these 3 dyes, based on their RGB components, resulting in separate images for each dye. An automated threshold method implemented in Matlab (Mathworks, Natick, MA, USA) was then applied to single-color images to differentiate foreground and background pixels using the method of Otsu (30). The colocalization ratios were computed as the total amount of common foreground pixels of 2 colors over the total amount of foreground pixels of each color. An observer unaware of histological classification and staining of the samples performed this analysis.

Immunofluorescence labeling was performed as described (31). In brief, sections were incubated overnight with mouse anti-mCRP (clone 9C9) and goat anti-Trx (American Diagnostica, Stamford, CT, USA) mAbs at 4°C in a humidified chamber. After 3 washes with PBS, sections were incubated with a solution containing amino-methyl-coumarin-acetate (AMCA)-coupled rabbit anti-goat IgG (Millipore, Billerica, MA, USA), Cy5-conjugated donkey anti-mouse IgG (Millipore), and Alexa-488-conjugated anti-E-cadherin Ab (Cell Signaling, Danvers, MA, USA) for 1 h at room temperature in a dark humidified chamber. Following 3 washes, sections were mounted on coverslips in mounting medium (Vector Laboratories). Images were captured in a Leica DMRI fluorescence microscope equipped with a digital camera (Retiga EX; QImaging, Surrey, BC, Canada) and OpenLab software (OpenLab Srl, Florence, Italy).

Statistical analysis

Data are presented as means ± SE. Statistical analysis was performed by the Mann-Whitney U test or Kruskal-Wallis ANOVA using ranks. Values of $P < 0.05$ were considered significant.

RESULTS

Intrasubunit disulfide bond is redox sensitive in mCRP but not pCRP

The redox-controlled thiol/disulfide exchange, or "sulfur switch," is a major regulatory mechanism operating in many biological processes (32). Since each human CRP subunit possesses 2 Cys residues (Cys36 and Cys97) that form an intrasubunit disulfide bond, we asked whether this bond was redox sensitive. Nonreducing SDS-PAGE and mass spectrometry analysis showed that the reducing agents DTT, GSH, or Cys did not reduce pCRP, not even after prolonged treatment (Fig. 1*A*). Indeed, the disulfide bond is packed inside the pCRP subunit (33), thereby preventing the access of exogenous reductants. By contrast, DTT, GSH, and Cys effectively reduced the disulfide bridge in mCRP (Fig. 1*A*, *B* and Supplemental Fig. S1). Moreover, following removal of the reducing agent *via* dialysis, the reduced Cys in mCRP underwent spontaneous reoxidation with the intrasubunit disulfide bond as the single product (Fig. 1*C*). These findings indicate that conformational rearrangement in pCRP, yielding mCRP, is required for reversible redox regulation of the intrasubunit disulfide bond.

Reducing the intrasubunit disulfide bond enhances mCRP binding to complement C1q but not to LDL

Since dissociation of pCRP to mCRP is associated with significantly enhanced capacity to bind LDL (24) and activate complement (25), we investigated the effect of reduction of the disulfide bond on these interactions. Reduced mCRP exhibited LDL interacting capacity comparable to that of nonreduced mCRP (**Fig. 2*A***). Nonreduced mCRP avidly bound C1q and effectively activated complement *via* the classic pathway; however, reduction of the disulfide bond in mCRP further enhanced these activities (Fig. 2*B*, *C*). The increased
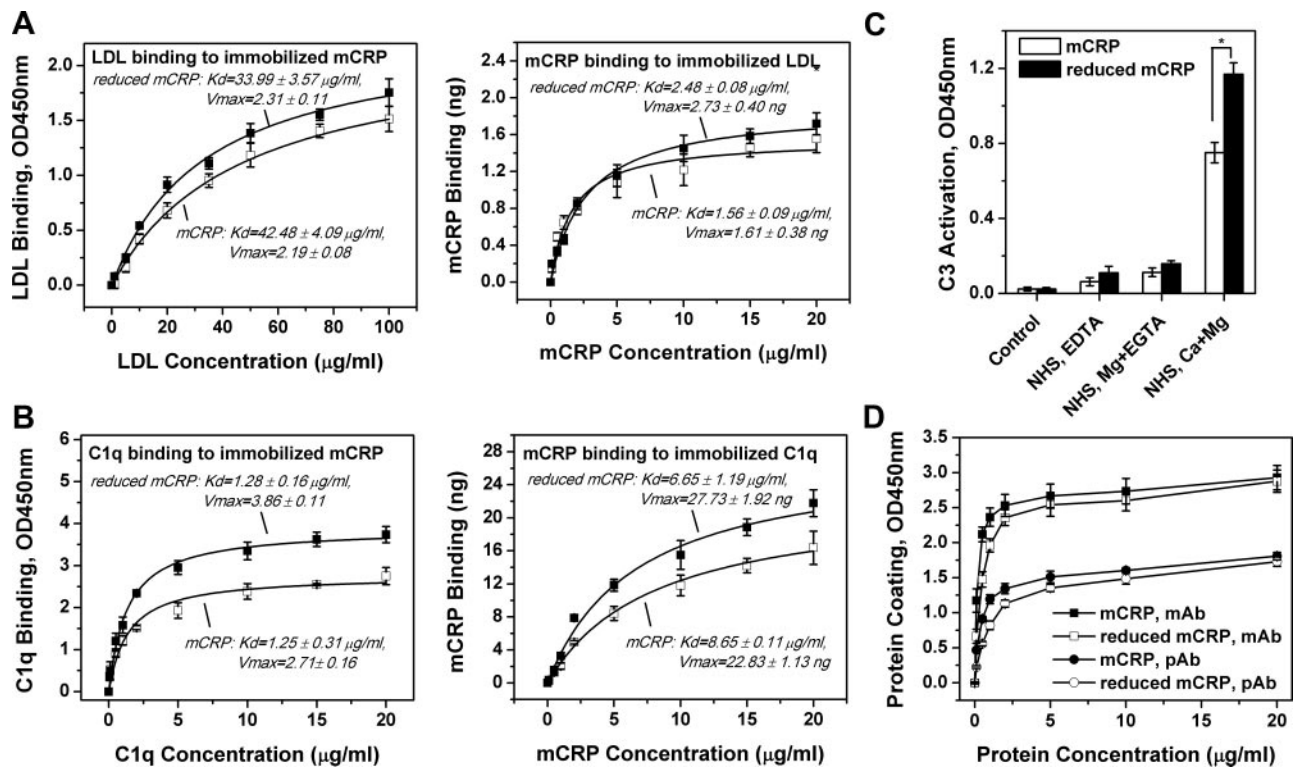
Figure 2. Reduction of the intrasubunit disulfide bond enhances mCRP binding to complement C1q. *A, B*) Interaction of untreated or DTT-treated mCRP in solid phase (left panel) or fluid phase (right panel) with LDL (*A*) and C1q (*B*) was assayed by ELISA (*n*=7). *C*) NHS (2%) was incubated with immobilized untreated or DTT-treated mCRP (5 μg/ml) in the presence of 0.15 mM Ca^{2+} plus 0.5 mM Mg^{2+}, 5 mM EGTA plus 0.5 mM Mg^{2+} (to block activation of the classical complement pathway), or 5 mM EDTA (to block complement activation). Complement activation was determined by C3d deposition (*n*=5). *D*) Coating efficiency of untreated and DTT-treated mCRP was determined by the anti-mCRP mAb 3H12 and an anti-CRP polyclonal antibody (anti-CRP pAb), respectively (*n*=3). Reduced and nonreduced mCRP showed comparable coating at 5 μg/ml.

complement-activating capacity of reduced mCRP was not due to higher coating when immobilized at 5 μg/ml (Fig. 2*D*). Taken together, these results indicate that irrespective of its redox states, mCRP is able to interact with LDL and C1q, and to activate the complement cascade.

Reducing the intrasubunit disulfide bond in mCRP markedly enhances its capacity to stimulate HCAECs

Since endothelial cell activation is a critical event in the development of coronary artery disease, we compared responses of HCAECs to nonreduced and reduced mCRP. Consistent with a previous report (19), nonreduced mCRP at concentrations up to 100 μg/ml was essentially inert in evoking HCAEC responses within 4 h incubation (**Fig. 3*A***). By contrast, reduction of the disulfide bond by DTT, GSH, or Cys, or mutation of Cys residues to Ala in mCRP (Cys-mutated mCRP), yielded molecules with markedly enhanced potency in inducing IL-8 and MCP-1 release (Fig. 3). For instance, reduced mCRP at a concentration as low as 1 μg/ml produced ~50% increase in cytokine production, suggesting that even low-throughput reduction of mCRP may be sufficient to exert significant biological activities under pathological conditions. Treatment of mCRP with oxidized DTT, GSH-disulfide, or cystine failed to

augment its biological activities (Fig. 3*B*). Furthermore, the stimulatory effects of LPS and PMA on HCAECs were mildly suppressed rather than enhanced in the presence of reducing agents (Fig. 3*C*). More important, Cys-mutated (*i.e.*, disulfide bond-free) mCRP was constitutively active in stimulating HCAECs (Fig. 3*C*). In SDS-PAGE, Cys-mutated mCRP migrated at the same position as reduced mCRP (Fig. 1*A*), and its biological activities were similar in the absence or presence of reducing agents (Fig. 3*C*). Of note, like native pCRP (13, 17, 19), DTT-treated pCRP did not evoke detectable changes in cytokine release within 4 h incubation (data not shown). Thus, the augmented HCAEC responses to reduced mCRP can be attributed to breakage of the intrasubunit disulfide bond rather than to other actions of the reducing agents.

Trx reduces mCRP and colocalizes with mCRP in human coronary artery atherosclerotic plaques

Trx is the central component of the intracellular thiol/disulfide redox system (20). Accumulating evidence also indicates important roles for extracellular Trx, including cytokine-like actions (34). Our results demonstrate that Trx can also effectively reduce mCRP (**Fig. 4*A***). On a molar basis, Trx was 1000-fold more efficient than DTT, GSH, or Cys. Consistent with results
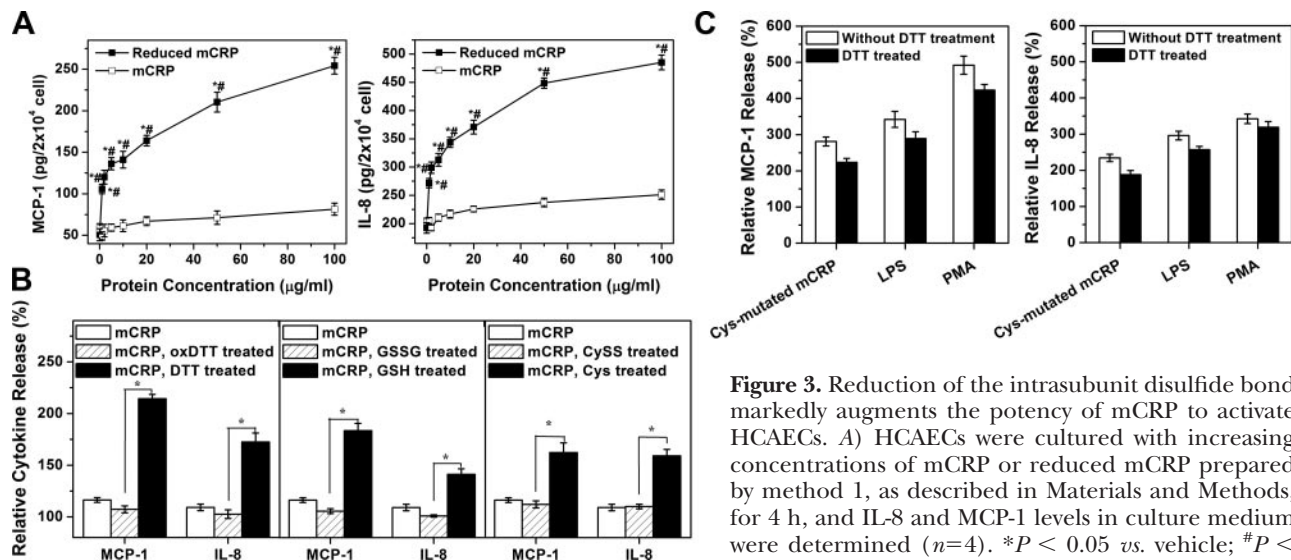
Figure 3. Reduction of the intrasubunit disulfide bond markedly augments the potency of mCRP to activate HCAECs. *A*) HCAECs were cultured with increasing concentrations of mCRP or reduced mCRP prepared by method 1, as described in Materials and Methods, for 4 h, and IL-8 and MCP-1 levels in culture medium were determined ($n=4$). *$P < 0.05$ *vs.* vehicle; #$P < 0.05$ *vs.* nonreduced mCRP. *B*) Cytokine release from HCAECs cultured for 4 h with 20 μg/ml mCRP pretreated with DTT (5 mM), GSH (20 mM), or Cys (20 mM) or their oxidized counterparts, *i.e.*, oxidized DTT (oxDTT), GSH-disulfide (GSSG), and cystine (CySS) ($n=6$). *$P < 0.05$. *C*) Cytokine release from HCAECs cultured for 4 h with Cys-mutated mCRP (20 μg/ml), PMA (100 nM), or LPS (2 μg/ml) with or without 5 mM DTT pretreatment. IL-8 and MCP-1 levels were measured in culture medium and expressed as fold increase compared to vehicle control ($n=4$).

obtained with other reducing agents, Trx treatment markedly enhanced the bioactivities of mCRP, but had no effect on Cys-mutated mCRP (Fig. 4*B*). Using CRP isoform-selective antibodies, we detected mCRP but not pCRP in human coronary artery atherosclerotic lesions, whereas apparently healthy coronary artery segments did not stain for mCRP or pCRP (Fig. 4*C*). Furthermore, mCRP staining frequently coincides with staining for Trx within advanced atherosclerotic lesions (Fig. 4*C*). Analysis with the ImageJ software revealed that 35.8–78.6% of mCRP-positive areas also stained positive for Trx ($n=6$). Both mCRP and Trx staining were predominantly localized extracellularly (Fig. 4*D*), suggesting that mCRP reduction by Trx may occur within the unstable plaque.

Reduction of the disulfide bridge in mCRP unlocks the cholesterol-binding sequence

To address the mechanism by which reduction of the disulfide bridge resulted in a more active mCRP form, we assessed reduction-induced conformational changes. Reduced mCRP exhibited nearly unaltered CD spectrum, mildly enhanced intrinsic fluorescence (~12%) and significantly increased ANS fluorescence (~37%) (**Fig. 5*A–C***). These findings indicate that reduction of the disulfide bond does not evoke overt changes in the gross structure of mCRP; rather, it primarily results in relaxation of local packing, presumably due to breakage of the constraint imposed by the intrasubunit disulfide bridge. This implies a critical role of sequence around the Cys in mediating reduction-associated functional alterations. Because Cys36 resides within the cholesterol-binding sequence (*i.e.*, aa 35–47) that mediates mCRP stimulation of endothelial cells

through interaction with lipid rafts (28), we reasoned that unlocking of the cholesterol-binding sequence was most likely responsible for translating reduction-induced trivial structural changes to significant mCRP cell stimulation activity. Indeed, breaking the disulfide bond by reducing agents or mutating the two Cyss significantly enhanced the interaction of mCRP with lipid rafts in both model and HCAEC membranes (Fig. 5*D*), consistent with the remarkably enhanced responses of HCAEC to reduced mCRP.

Sequence alignment of CRPs from various species (Supplemental Fig. S2*A*) and homology modeling (Supplemental Fig. S2*B*) revealed that Cys36 and Cys97 of human CRP, the intrasubunit disulfide bond, and the Cys-containing cholesterol-binding sequence (**L/V-C-X$_{(0-3)}$-Y-X$_{(2-6)}$-R/K**; Supplemental Fig. S2*A*) are invariant throughout the evolution, highlighting an important and a conserved role for the disulfide bond in the structure and function of CRP. Consistent with this notion, reduction of the disulfide bridge was also required for rabbit mCRP to induce IL-8 and MCP-1 release from HCAECs (Supplemental Fig. S2*C*).

Reduction of the disulfide bridge enhances the proinflammatory actions of mCRP *in vitro* and *in vivo*

Next, we compared the biological activities of reduced and nonreduced mCRP. Reduced mCRP was more potent than nonreduced mCRP to induce ROS production in HCAECs (**Fig. 6*A***); to up-regulate expression of VCAM-1, ICAM-1, and E-selectin (Fig. 6*B*); and to enhance monocyte adhesion to HCAECs (Fig. 6*C*). Moreover, reduced mCRP evoked considerably higher IL-8 and IL-6 release from rabbit thoracic aorta *ex vivo* (Fig. 6*D*) and in mice than nonreduced mCRP (Fig.
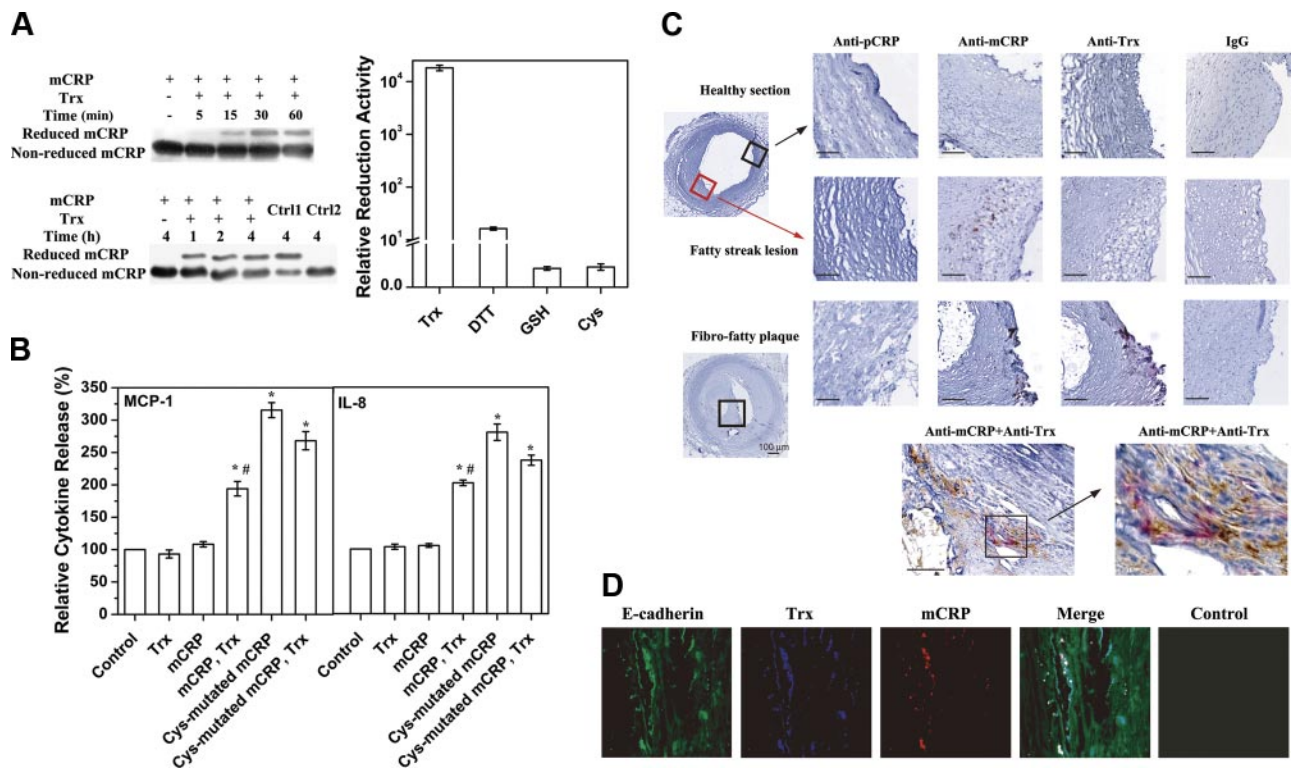
Figure 4. Trx regulation of the structure and actions of mCRP. *A*) Reduction of the disulfide bridge by Trx. mCRP (10 or 20 μg/ml; ~0.43 or 0.86 μM) was incubated with 20 μg/ml (~1.57 μM) reduced Trx (Trx pretreated with 5 mM DTT for 40 min) for the indicated time periods, and then subjected to nonreducing SDS-PAGE followed by immunoblotting. DTT at a concentration present in reduced Trx preparation did not produce detectable reduction of mCRP. mCRP treated with DTT (5 mM; Ctrl 1) and pCRP treated with Trx (20 μg/ml for 4 h; Ctrl 2) served as controls. During the assay, 2 mM Ca^{2+} was present. Relative reduction activities were calculated as percentage of reduced mCRP × 10^3/molar ratio of reducing agents to mCRP substrate. Determination of free thiols in mCRP before and after reduction revealed that 19.8 ± 2.4% of mCRP was reduced by Trx (*n*=4). *B*) Cytokine release from HCAECs cultured for 4 h with mCRP treated with Trx (5 μg/ml for 30 min; *n*=3). *$P <$ 0.05 *vs.* control; $^#P <$ 0.05 *vs.* nonreduced mCRP. *C*) Detection of mCRP and Trx in human coronary artery plaques. Frozen human coronary artery segments (6-μm sections) were stained with antibodies that recognize pCRP (clone 8D8), mCRP (clone 9C9), or Trx, followed by a goat anti-mouse HRP-conjugated antibody. Slides were incubated with an avidin-biotin-peroxidase system; reaction products were stained with DAB (for mCRP and CRP) and Fast Red (for Trx) and then counterstained with hematoxylin. Staining with isotype-matched nonspecific mouse IgG plus DAB or Fast Red served as controls. Results are representative for 6 samples from different donors. High-power fields show double immunostaining of fibrofatty plaque sample for mCRP (brown) and Trx (red). Scale bars = 100 μm. *D*) Triple-staining immunofluorescence for E-cadherin (green), Trx (blue), and mCRP (red) in fibrofatty plaques. Control was stained with secondary antibodies only. Images were captured in a Leica DMRI fluorescence microscope equipped with a Retiga EX digital camera and OpenLab software. Results are representative of 3 samples from different donors.

6*E*). Taken together, these data establish the intrasubunit disulfide bond as an important switch that controls the structure and bioactivities of mCRP both *in vitro* and *in vivo*, the reduction of which enhances the interaction of mCRP with membrane lipid raft microdomains *via* exposure of the cholesterol-binding motif.

DISCUSSION

CRP has been implicated in multiple aspects of atherogenesis and plaque vulnerability. Accumulating evidence indicates that the structure of CRP profoundly affects its actions; however, little is known of how the CRP actions are regulated. In the present study, we identified the intrasubunit disulfide bridge as a redox-

sensitive switch whose reduction is required for the expression of potent proinflammatory actions once the pentameric symmetry in pCRP is lost.

Although CRP immunoreactivity and mRNA have been detected in atherosclerotic lesions (1–3, 9, 35), it is still uncertain which CRP isoform is predominant, because the widely used anti-CRP antibodies recognize both pCRP and mCRP (9). Presence of calcium is thought to prevent pCRP→mCRP conversion (1). However, binding of pCRP to activated platelets (16) and damaged cell membranes (17) results in rapid dissociation of pCRP into mCRP even in the presence of calcium. Indeed, recent immunohistochemical studies using selective mAbs to pCRP and mCRP detected mCRP, rather than pCRP, in human aortic atherosclerotic plaques (16), and this was confirmed in early and advanced coronary artery plaques in the present study.
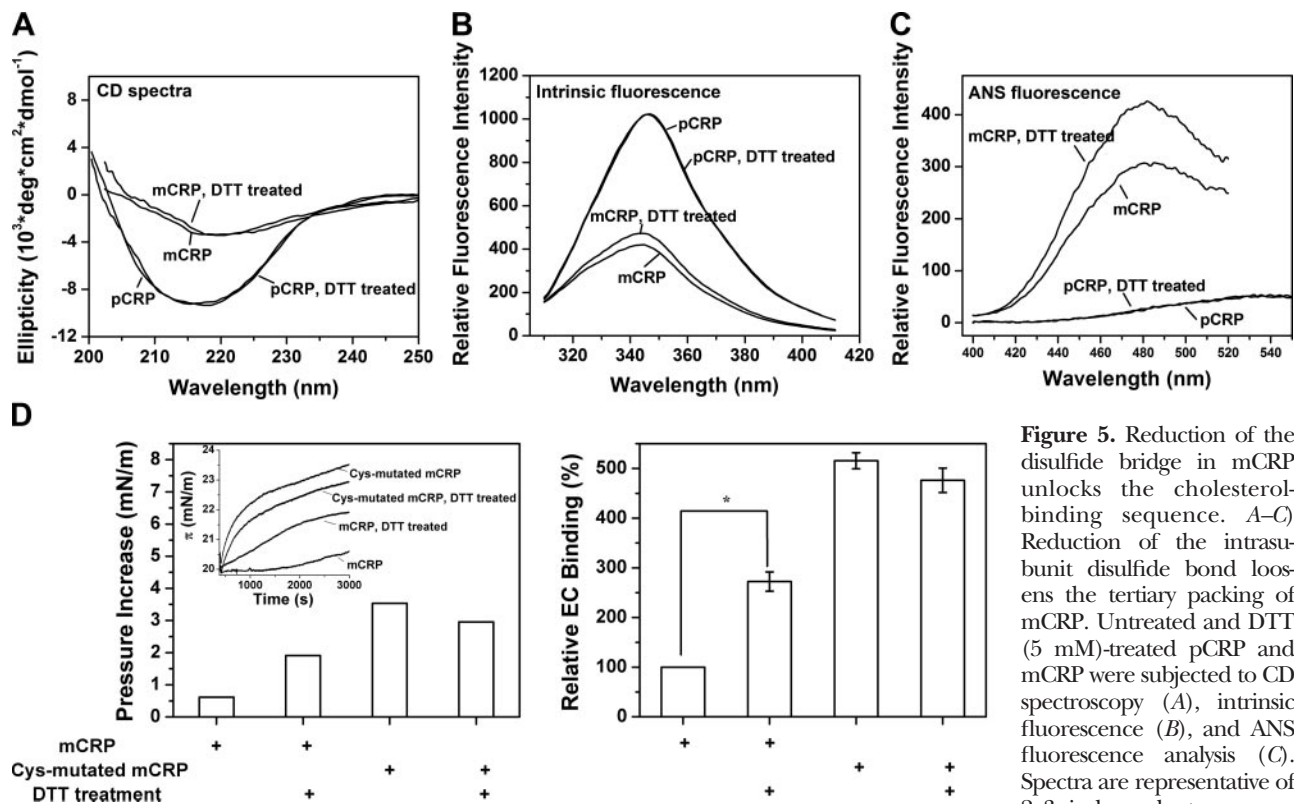
Figure 5. Reduction of the disulfide bridge in mCRP unlocks the cholesterol-binding sequence. *A–C*) Reduction of the intrasubunit disulfide bond loosens the tertiary packing of mCRP. Untreated and DTT (5 mM)-treated pCRP and mCRP were subjected to CD spectroscopy (*A*), intrinsic fluorescence (*B*), and ANS fluorescence analysis (*C*). Spectra are representative of 2–3 independent measurements. *D*) Membrane insertion and HCAEC binding of untreated, DTT-treated, or Cys-mutated mCRP (n=3–5). Proteins were labeled with FITC in the HCAEC binding assay. *$P < 0.05$.

The weak signal or even absence of pCRP would suggest the lability of this protein in the inflammatory microenvironment. We cannot exclude the possibility that the conformational determinants in pCRP might partially be altered or occupied by ligands (such as PC or C1q), leading to failure of detection by relevant mAbs; nonetheless, these findings would indicate involvement of mCRP rather than pCRP in progression of atherosclerotic lesions.

Evolutionary conservation of the disulfide bond forming Cys in CRP (Cys36 and Cys97) hints at the importance of this feature at the structural and/or functional level. Because of the compact fold of the pCRP subunit (33), conformational rearrangement to mCRP with significantly relaxed tertiary packing is the prerequisite for the disulfide bond to be accessible by physiological reductants, such as Trx, GSH, and Cys. Our data show that reduction of the disulfide bridge results in mild structural changes in mCRP concomitant with moderately enhanced interactions with complement. The most striking consequence of reduction of mCRP is the remarkable augmentation of its potency to stimulate IL-8 and MCP-1 production and ROS generation in HCAECs; to induce adhesion molecule expression on HCAECs, thereby promoting monocyte-HCAEC adhesion; and to evoke release of IL-8 and IL-6 *ex vivo* and *in vivo*, respectively. Likewise, removal of the disulfide bond by mutating Cys to Ala yields a molecule with biological activities comparable to those of reduced mCRP. These observations thus identify the intrasubunit disulfide bridge as a redox-sensitive switch

that controls the structure as well as the biological activities of CRP. The redox state of this switch may also explain the reported differences in endothelial cell responses to nonreduced mCRP (18–19) and Cys-mutated mCRP (13, 28). Moreover, the function of mCRP might have been affected by the presence of reducing agents, common constituents of culture medium, under certain experimental conditions.

While mCRP binds CD16 on phagocytes (26), we have previously shown that HCAEC responses to mCRP are predominantly mediated through interaction of a cholesterol-binding sequence in the CRP subunit with cholesterol-rich lipid rafts of plasma membranes (28). Since Cys36 is located within the cholesterol-binding sequence (aa 35–47), it is plausible that the full functionality of the cholesterol-binding sequence depends on the release of the structural constraint imposed by the disulfide bridge formed between Cys36 and Cys97. Consistently, reduction of the disulfide bond significantly enhanced mCRP binding to endothelial cell lipid raft membranes; while disrupting lipid rafts abrogated binding of both reduced mCRP and Cys-mutated mCRP to HCAEC as well as HCAEC responses to these modified proteins. Moreover, our conservation analysis and experiments with human and rabbit mCRP orthologs suggest that lipid raft binding and redox regulation are evolutionarily conserved mechanisms critical for modulation of the structure and function of CRP.

Sulfur switch is an essential component of redox regulation (32), as documented by the redox-sensitive activities of the transcription factors AP-1 and NF-κB,
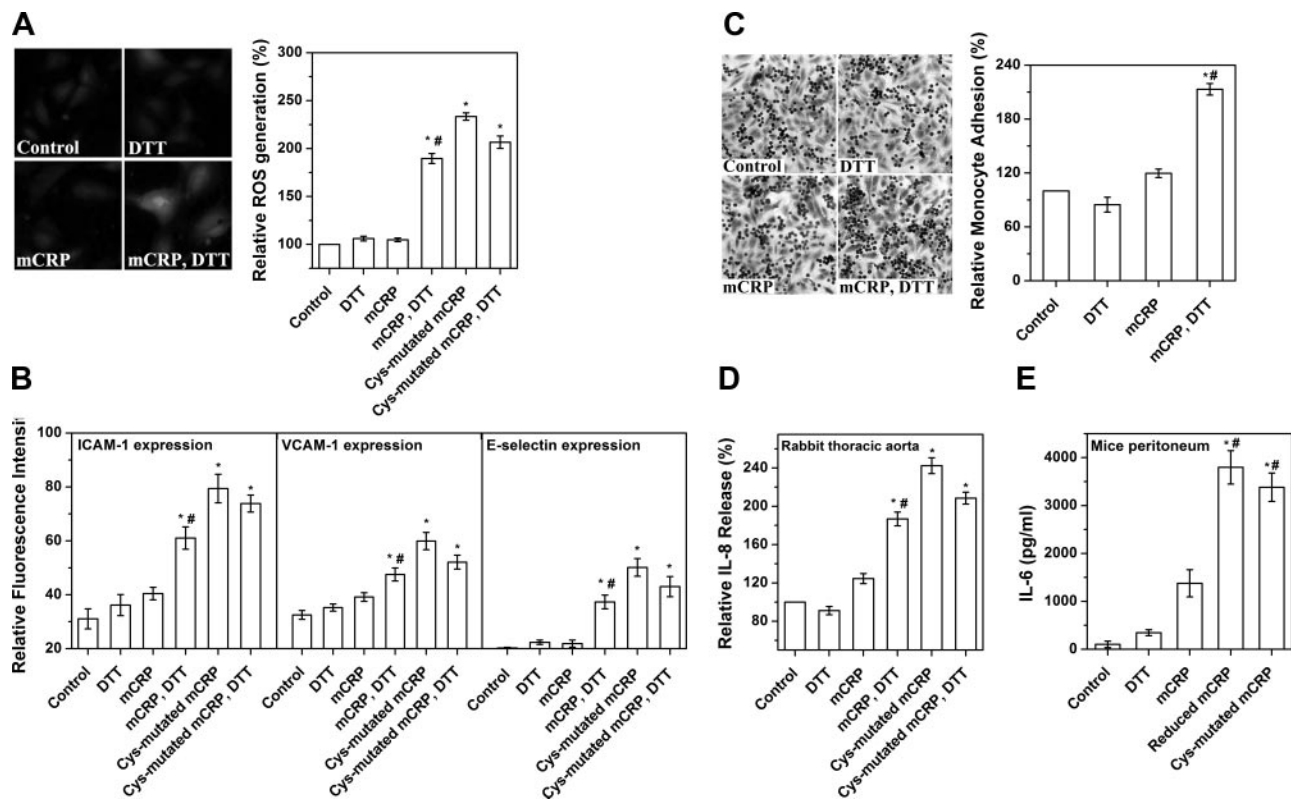
Figure 6. Enhanced responses to reduced mCRP *in vitro, ex vivo* and *in vivo. A*) Generation of ROS by HCAECs. HCAEC monolayers were incubated with vehicle, untreated mCRP, or mCRP treated with 5 mM DTT (20 μg/ml) for 2 h, then 10 μM H$_2$DCF-DA was added for an additional 30 min to assess ROS generation (*n*=3). *B*) Expression of VCAM-1, ICAM-1, and E-selectin. HCAECs were cultured for 4 h with vehicle, mCRP, or reduced mCRP (20 μg/ml). Adhesion molecule expression was assessed by staining with specific antibodies followed by a fluorescent dye-conjugated secondary antibody (*n*=6). *C*) Monocyte adhesion to HCAECs. HCAECs were stimulated for 4 h with mCRP or reduced mCRP (20 μg/ml). After washing, PMA-activated U937 monocytes were added for 30 min. Cells were stained with crystal violet and photographed, and adherent monocytes were counted (*n*=3). *D*) IL-8 release from rabbit aorta. Rabbit thoracic aorta segments were cultured for 4 h with 50 μg/ml mCRP or reduced mCRP. IL-8 release was determined with specific ELISA (*n*=4). *E*) IL-6 release from mouse peritoneum. Male Kunming mice were injected intraperitoneally with human mCRP, reduced mCRP, or Cys-mutated mCRP (2.5 mg/kg). At 2 h postinjection, the peritoneum was perfused, and IL-6 concentrations were determined (*n*=6–8). *$P < 0.05$ *vs.* control; #$P < 0.05$ *vs.* untreated mCRP.

the chaperone Hsp33, the cation channel TRPC (36), angiotensinogen (37) and β-defensin 1 (38). We show here that CRP, the prototypic acute-phase reactant, also possesses such a switch (*i.e.*, Cys36), expressing an on state in the reduced form. It may appear paradoxical that reduction of mCRP could occur in the oxidative inflammatory microenvironment, such as the atherosclerotic plaque. However, reduced mCRP could activate HCAECs at concentrations <1 μg/ml *in vitro*, suggesting that even small amounts of reduced mCRP are likely sufficient to evoke pronounced endothelial responses *in situ*. Moreover, mCRP generated from pCRP predominantly occurs on damaged or activated cell membranes (16–17), favoring local accumulation of mCRP and its subsequent reduction by secreted and/or membrane-associated Trx (39). Indeed, our immunohistochemistry and immunofluorescence studies demonstrating frequent colocalization of Trx with mCRP at the cell surface in the intima of human advanced atherosclerotic plaques support this notion and suggest that Trx-mediated activation of the sulfur switch in mCRP would likely occur *in vivo*. However,

direct proof of its occurrence *in vivo* awaits development of a specific marker to identify the reduced form of mCRP. Of note, extracellular Trx is an emerging biomarker of inflammation (20, 40) and unstable angina (41). Increased extracellular Trx expression has been detected in coronary culprit lesions in patients with unstable angina (42). Macrophages and vascular cells release Trx in response to proatherogenic molecules, such as oxidized LDL (21, 39). In addition, other extracellular reductants (*e.g.*, Cys and GSH) and secreted or cell surface reductase (*e.g.*, Grx) may also contribute to the reduction of mCRP.

Trx has been shown to function as a costimulator with TNF-α to activate fibroblasts (34). It remains to be investigated whether Trx could also synergize with reduced mCRP, though our data show that reduced mCRP is sufficient to evoke robust HCAEC responses in the absence of Trx. Low-level Trx expression in early atherosclerotic lesions would suggest that mCRP reduction might more likely occur in vulnerable plaques. mCRP promotes recruitment of monocytes/macrophages (16), the predominant source of Trx, thereby

Figure 7. Proposed 2-step model for the structure/activity interplay of CRP isoforms during inflammation underlying coronary artery disease. First, pCRP undergoes conformational changes to dissociate into mCRP. Irrespective of its redox state, mCRP may regulate LDL metabolism and complement activation. Second, reduction of the intrasubunit disulfide bridge removes additional structural constraints in mCRP posed by the disulfide bond and unlocks the cholesterol-binding sequence, thereby unmasking potent proinflammatory actions on endothelial and other cells.
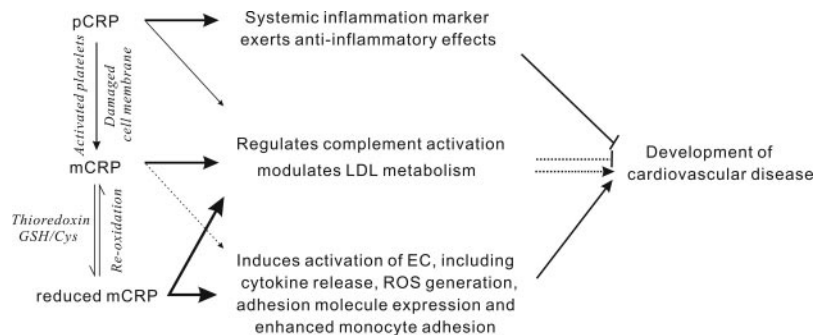
forming a vicious circle that may trigger acute coronary events. The limited availability of human coronary artery specimens precluded direct assessment of the presence of reduced mCRP. However, we detected cell-associated mCRP reduction by COS-7 cells transfected with GFP-Trx (unpublished results). Trx is generally thought to exert anti-inflammatory actions, however, it also possesses potent proinflammatory activities. For instance, extracellular Trx contributes to the progression of arthritis *via* reduction of TRPC channel (36), and inhibition of Trx/Trx reductase is beneficial in certain cancers (43). We thus propose that Trx regulation of the redox state of mCRP is another mechanism that may tip the balance of its pro- and anti-inflammatory activities under pathological conditions. Interestingly, Trx desensitize monocytes to MCP-1 but not IL-8 (44), further highlighting the intricate interplay among various factors within inflammatory loci.

Based on previous and our present findings, we propose a two-step model for the expression of proinflammatory actions in pCRP (**Fig. 7**). First, pCRP undergoes conformational changes to dissociate into mCRP, which exhibits altered ligand recognition and interaction capacity (9, 24–25). Irrespective to its redox state, mCRP may regulate LDL metabolism (24, 45) and complement activation (25), likely exerting atheroprotective actions, in particular at initial stages of lesion development (46) by enhancing innate immunity and the clearance of the damaged cells. Second, reduction of the intrasubunit disulfide bridge removes additional structural constraints on mCRP posed by the disulfide bond and unlocks the cholesterol-binding sequence, thereby unmasking proinflammatory activities, which may accelerate disease progression and trigger acute events. The actions of reduced mCRP might, however, be limited by proteolysis and Cys→disulfide reoxidation. Therefore, interpretation of the role of CRP in cardiovascular disease should take into account the highly context-dependent interplay between the biological actions of different structural states of CRP isoforms.

In summary, our study identifies the intrasubunit disulfide bridge in CRP as a redox switch that profoundly affects its biological properties. However, this switch can only be activated following loss of pentameric structure in CRP. Native pCRP can rapidly dissociate into mCRP on the surface of damaged or activated

cells and thus can be exposed to Trx or other reducing agents at sites of inflammation. This 2-step regulatory mechanism would then ensure prompt and localized responses, uncoupling the local effective concentration of mCRP from circulating levels of pCRP, and would determine the expression of anti- or proinflammatory activities of pCRP, mCRP, and reduced mCRP during inflammation. These multiple layers of regulation would underlie the intrinsic competence of CRP as a fine modulator of activation of endothelial and other cells to adjust the intensity of local inflammation, ultimately contributing to progression of atherosclerosis and development of unstable plaques in the coronary artery. ◻

REFERENCES

1. Pepys, M. B., and Hirschfield, G. M. (2003) C-reactive protein: a critical update. *J. Clin. Invest.* **111,** 1805–1812
2. Singh, S. K., Suresh, M. V., Voleti, B., and Agrawal, A. (2008) The connection between C-reactive protein and atherosclerosis. *Ann. Med.* **40,** 110–120
3. Verma, S., Devaraj, S., and Jialal, I. (2006) C-reactive protein promotes atherothrombosis. *Circulation* **113,** 2135–2151
4. Paul, A., Ko, K. W., Li, L., Yechoor, V., McCrory, M. A., Szalai, A. J., and Chan, L. (2004) C-reactive protein accelerates the progression of atherosclerosis in apolipoprotein E-deficient mice. *Circulation* **109,** 647–655
5. Hirschfield, G. M., Gallimore, J. R., Kahan, M. C., Hutchinson, W. L., Sabin, C. A., Benson, G. M., Dhillon, A. P., Tennent, G. A., and Pepys, M. B. (2005) Transgenic human C-reactive protein is not proatherogenic in apolipoprotein E-deficient mice. *Proc. Natl. Acad. Sci. U. S. A.* **102,** 8309–8314
6. Kovacs, A., Tornvall, P., Nilsson, R., Tegner, J., Hamsten, A., and Bjorkgren, J. (2007) Human C-reactive protein slows atherosclerosis development in a mouse model with human-like hypercholesterolemia. *Proc. Natl. Acad. Sci. U. S. A.* **104,** 13768–13773
7. Teupser, D., Weber, O., Rao, T. N., Sass, K., Thiery, J., and Fehling, H. J. (2011) No reduction of atherosclerosis in C-reactive protein (CRP)-deficient mice. *J. Biol. Chem.* **286,** 6272–6279
8. Koike, T., Kitajima, S., Yu, Y., Nishijima, K., Zhang, J., Ozaki, Y., Morimoto, M., Watanabe, T., Bhakdi, S., Asada, Y., Chen, Y. E., and Fan, J. (2009) Human C-reactive protein does not promote atherosclerosis in transgenic rabbits. *Circulation* **120,** 2088–2094

9. Schwedler, S. B., Filep, J. G., Galle, J., Wanner, C., and Potempa, L. A. (2006) C-reactive protein: a family of proteins to regulate cardiovascular function. *Am. J. Kidney Dis.* **47,** 212–222

10. Filep, J. G. (2009) Platelets affect the structure and function of C-reactive protein. *Circ. Res.* **105,** 109–111

11. Zhao, J., Ji, S. R., and Wu, Y. (2010) C-reactive protein – a link between cardiovascular disease and inflammation. *Acta Biophys. Sinica* **26,** 87–96

12. Ciubotaru, I., Potempa, L. A., and Wander, R. C. (2005) Production of modified C-reactive protein in U937-derived macrophages. *Exp. Biol. Med. (Maywood)* **230,** 762–770

13. Khreiss, T., Jozsef, L., Potempa, L. A., and Filep, J. G. (2004) Conformational rearrangement in C-reactive protein is required for proinflammatory actions on human endothelial cells. *Circulation* **109,** 2016–2022

14. Khreiss, T., Jozsef, L., Potempa, L. A., and Filep, J. G. (2005) Loss of pentameric symmetry in C-reactive protein induces interleukin-8 secretion through peroxynitrite signaling in human neutrophils. *Circ. Res.* **97,** 690–697

15. Molins, B., Pena, E., Vilahur, G., Mendieta, C., Slevin, M., and Badimon, L. (2008) C-reactive protein isoforms differ in their effects on thrombus growth. *Arterioscler. Thromb. Vasc. Biol.* **28,** 2239–2246

16. Eisenhardt, S. U., Habersberger, J., Murphy, A., Chen, Y. C., Woollard, K. J., Bassler, N., Qian, H., von Zur Muhlen, C., Hagemeyer, C. E., Ahrens, I., Chin-Dusting, J., Bobik, A., and Peter, K. (2009) Dissociation of pentameric to monomeric C-reactive protein on activated platelets localizes inflammation to atherosclerotic plaques. *Circ. Res.* **105,** 128–137

17. Ji, S. R., Wu, Y., Zhu, L., Potempa, L. A., Sheng, F. L., Lu, W., and Zhao, J. (2007) Cell membranes and liposomes dissociate C-reactive protein (CRP) to form a new, biologically active structural intermediate: mCRP (m). *FASEB J.* **21,** 284–294

18. Devaraj, S., Venugopal, S., and Jialal, I. (2006) Native pentameric C-reactive protein displays more potent pro-atherogenic activities in human aortic endothelial cells than modified C-reactive protein. *Atherosclerosis* **184,** 48–52

19. Taylor, K. E., and van den Berg, C. W. (2007) Structural and functional comparison of native pentameric, denatured monomeric and biotinylated C-reactive protein. *Immunology* **120,** 404–411

20. Hoshino, Y., Shioji, K., Nakamura, H., Masutani, H., and Yodoi, J. (2007) From oxygen sensing to heart failure: role of thioredoxin. *Antioxid. Redox Signal.* **9,** 689–699

21. Yamawaki, H., Haendeler, J., and Berk, B. C. (2003) Thioredoxin: a key regulator of cardiovascular homeostasis. *Circ. Res.* **93,** 1029–1033

22. Potempa, L. A., Maldonado, B. A., Laurent, P., Zemel, E. S., and Gewurz, H. (1983) Antigenic, electrophoretic and binding alterations of human C-reactive protein modified selectively in the absence of calcium. *Mol. Immunol.* **20,** 1165–1175

23. Wu, Y., Ji, S. R., Wang, H. W., and Sui, S. F. (2002) Study of the spontaneous dissociation of rabbit C-reactive protein. *Biochemistry* **67,** 1377–1382

24. Ji, S. R., Wu, Y., Potempa, L. A., Qiu, Q., and Zhao, J. (2006) Interactions of C-reactive protein with low density lipoproteins: implications for an active role of modified C-reactive protein in atherosclerosis. *Int. J. Biochem. Cell Biol.* **38,** 648–661

25. Ji, S. R., Wu, Y., Potempa, L. A., Liang, Y. H., and Zhao, J. (2006) Effect of Modified C-reactive protein on complement activation. A possible complement regulatory role of modified or monomeric C-reactive protein in atherosclerotic lesions. *Arterioscler. Thromb. Vasc. Biol.* **26,** 935–941

26. Heuertz, R. M., Schneider, G. P., Potempa, L. A., and Webster, R. O. (2005) Native and modified C-reactive protein bind different receptors on human neutrophils. *Int. J. Biochem. Cell Biol.* **37,** 320–335

27. Ying, S. C., Gewurz, H., Kinoshita, C. M., Potempa, L. A., and Siegel, J. N. (1989) Identification and partial characterization of multiple native and neoantigenic epitopes of human C-reactive protein by using monoclonal antibodies. *J. Immunol.* **143,** 221–228

28. Ji, S. R., Ma, L., Bai, C. J., Shi, J. M., Li, H. Y., Potempa, L. A., Filep, J. G., Zhao, J., and Wu, Y. (2009) Monomeric C-reactive protein activates endothelial cells via interaction with lipid raft micro-domains. *FASEB J.* **23,** 1806–1816

29. Ruifrok, A. C., and Johnston, D. A. (2001) Quantification of histochemical staining by color deconvolution. *Anal. Quant. Cytol. Histol.* **23,** 291–299

30. Otsu, N. (1979) A threshold selection method from grey-level histograms. *IEEE Trans. Sys. Man. Cyber.* **9,** 62–66

31. Chatoo, W., Abdouh, M., David, J., Champagne, M. P., Ferreira, J., Rodier, F., and Bernier, G. (2009) The polycomb group gene Bmi1 regulates antioxidant defenses in neurons by repressing p53 pro-oxidant activity. *J. Neurosci.* **29,** 529–542

32. Kemp, M., Go, Y. M., and Jones, D. P. (2008) Nonequilibrium thermodynamics of thiol/disulfide redox systems: a perspective on redox systems biology. *Free Radic. Biol. Med.* **44,** 921–937

33. Shrive, A. K., Cheetham, G. M., Holden, D., Myles, D. A., Turnell, W. G., Volanakis, J. E., Pepys, M. B., Bloomer, A. C., and Greenhough, T. J. (1996) Three dimensional structure of human C-reactive protein. *Nat. Struct. Biol.* **3,** 346–354

34. Yoshida, S., Katoh, T., Tetsuka, T., Uno, K., Matsui, N., and Okamoto, T. (1999) Involvement of thioredoxin in rheumatoid arthritis: its costimulatory roles in the TNF-alpha-induced production of IL-6 and IL-8 from cultured synovial fibroblasts. *J. Immunol.* **163,** 351–358

35. Volanakis, J. E. (2001) Human C-reactive protein: expression, structure, and function. *Mol. Immunol.* **38,** 189–197

36. Xu, S. Z., Sukumar, P., Zeng, F., Li, J., Jairaman, A., English, A., Naylor, J., Ciurtin, C., Majeed, Y., Milligan, C. J., Bahnasi, Y. M., Al-Shawaf, E., Porter, K. E., Jiang, L. H., Emery, P., Sivaprasadarao, A., and Beech, D. J. (2008) TRPC channel activation by extracellular thioredoxin. *Nature* **451,** 69–72

37. Zhou, A., Carrell, R. W., Murphy, M. P., Wei, Z., Yan, Y., Stanley, P. L., Stein, P. E., Broughton Pipkin, F., and Read, R. J. (2010) A redox switch in angiotensinogen modulates angiotensin release. *Nature* **468,** 108–111

38. Schroeder, B. O., Wu, Z., Nuding, S., Groscurth, S., Marcinowski, M., Beisner, J., Buchner, J., Schaller, M., Stange, E. F., and Wehkamp, J. (2011) Reduction of disulphide bonds unmasks potent antimicrobial activity of human beta-defensin 1. *Nature* **469,** 419–423

39. Watanabe, R., Nakamura, H., Masutani, H., and Yodoi, J. (2010) Anti-oxidative, anti-cancer and anti-inflammatory actions by thioredoxin 1 and thioredoxin-binding protein-2. *Pharmacol. Ther.* **127,** 261–270

40. Burke-Gaffney, A., Callister, M. E., and Nakamura, H. (2005) Thioredoxin: friend or foe in human disease? *Trends Pharmacol. Sci.* **26,** 398–404

41. Miyamoto, S., Sakamoto, T., Soejima, H., Shimomura, H., Kajiwara, I., Kojima, S., Hokamaki, J., Sugiyama, S., Yoshimura, M., Ozaki, Y., Nakamura, H., Yodoi, J., and Ogawa, H. (2003) Plasma thioredoxin levels and platelet aggregability in patients with acute myocardial infarction. *Am. Heart J.* **146,** 465–471

42. Nishihira, K., Yamashita, A., Imamura, T., Hatakeyama, K., Sato, Y., Nakamura, H., Yodoi, J., Ogawa, H., Kitamura, K., and Asada, Y. (2008) Thioredoxin in coronary culprit lesions: possible relationship to oxidative stress and intraplaque hemorrhage. *Atherosclerosis* **201,** 360–367

43. Mukherjee, A., and Martin, S. G. (2008) The thioredoxin system: a key target in tumour and endothelial cells. *Br. J. Radiol.* **81**(Spec. 1), S57–S68

44. Pagliei, S., Ghezzi, P., Bizzarri, C., Sabbatini, V., Frascaroli, G., Sozzani, S., Caselli, G., and Bertini, R. (2002) Thioredoxin specifically cross-desensitizes monocytes to MCP-1. *Eur. Cytokine Netw.* **13,** 261–267

45. Schwedler, S. B., Hansen-Hagge, T., Reichert, M., Schmiedeke, D., Schneider, R., Galle, J., Potempa, L. A., Wanner, C., and Filep, J. G. (2009) Monomeric C-reactive protein decreases acetylated LDL uptake in human endothelial cells. *Clin. Chem.* **55,** 1728–1731

46. Schwedler, S. B., Amann, K., Wernicke, K., Krebs, A., Nauck, M., Wanner, C., Potempa, L. A., and Galle, J. (2005) Native C-reactive protein (CRP) increases, whereas modified CRP reduces atherosclerosis in ApoE-knockout-mice. *Circulation* **112,** 1016–1023